Application of longitudinal generalized magneto-optical ellipsometry in magnetic ultrathin films*

Wang Xiao(王 晓)[a], Lian Jie(连 洁)[a]†, Zhang Fu-Jun(张福军)[a], Gao Shang(高 尚)[a], Chen Yan-Xue(陈延学)[b], Yu Xiao-Hong(于晓红)[a], Li Ping(李 萍)[a], Wang Ying-Shun(王英顺)[a], and Sun Zhao-Zong(孙兆宗)[a]

[a] *Shandong University, Department of Optical Engineering, Jinan* 250100, *China*
[b] *Shandong University, School of Physics and Microelectronics, Jinan* 250100, *China*

(Received 9 May 2013; revised manuscript received 2 July 2013; published 3 December 2013)

The longitudinal generalized magneto-optical ellipsometry (GME) method is extended to the measurement of three-layer ultrathin magnetic films. In this work, the theory of the reflection matrix is introduced into the GME measurement to obtain the reflective matrix parameters of ultrathin multilayer magnetic films with different thicknesses. After that, a spectroscopic ellipsometry is used to determine the optical parameter and the thickness of every layer of these samples, then the magneto-optical coupling constant of the multilayer magnetic ultrathin film can be obtained. After measurements of a series of ultrathin Fe films, the results show that the magneto-optical coupling constant Q is independent of the thickness of the magnetic film. The magneto-optical Kerr rotations and ellipticity are measured to confirm the validity of this experiment. Combined with the optical constants and the Q constant, the Kerr rotations and ellipticity are calculated in theory. The results show that the theoretical curve fits very well with the experimental data.

Keywords: generalized magneto-optical ellimpsometry, magneto-optical coupling constant

PACS: 75.50.Bb, 78.20.Ls, 85.70.Sq **DOI:** 10.1088/1674-1056/23/1/017501

1. Introduction

Nowadays, magneto-optical ultrathin films have been widely used in the disk read–write area[1–4] and spinning electron devices. The development and implementation of spintronic devices require detailed information on the kinetic, relaxation and transport properties of spin subsystems.[5] Berger and Pufall proposed the generalized magneto-optical ellipsometry (GME)[6] as an experimental technique for the measurement of the complex magneto-optical coupling parameter Q of isotropic ferromagnetic bulk materials.[7] Now, the GME technique is further explored and can be used in many areas as a high precision test method.[8–11]

In this work, combined with Zak's reflection matrix[12,13] theory to calculate the reflective matrix of a three-layer system, the GME technique is extended to the measurement of ultra thin multilayer magnetic films. Unlike other techniques, by using the reflective matrix theory, the reflective index equations (r_{ss}, r_{sp}, r_{ps}, and r_{pp}) containing all the factors in every layer of the multilayer system can be obtained. From these equations, the influences of the optical parameter and the film thickness on the reflective index can be directly shown, so the relation between Q and material parameter can be given more accurately. The magneto-optical properties of Ta/Fe/GaAs(001) are also investigated using GME under a wavelength of 650 nm. The thicknesses of the Fe layers are 7.1 nm, 14.7 nm, 24.1 nm, 42.6 nm and 51.7 nm respectively. Our results show that the magneto-optical coupling constant is independent of the film thickness. The magneto-optical Kerr rotations are measured to confirm the consistence of the experiment. The theoretical data fit very well with the experimental results.

2. Theory

The interaction between light and the magnetized media is called the magneto-optical effect. The magnetic field will change the polarization of the incident light and the dielectric tensor. Then the magnetic field induced dielectric tensor can be expressed as[7]

$$\varepsilon = \begin{pmatrix} \varepsilon_x & \mathrm{i}Qm_z & \mathrm{i}Qm_y \\ -\mathrm{i}Qm_z & \varepsilon_y & \mathrm{i}Qm_x \\ -\mathrm{i}Qm_y & -\mathrm{i}Qm_x & \varepsilon_z \end{pmatrix}, \tag{1}$$

where m_x, m_y and m_z represent the normalized magnetization components in the x, y and z directions, respectively. For longitudinal magneto-optical effects, we have $m_x = m_y = 0$. The off-diagonal non-symmetric terms ε_{ij} $(i \neq j)$ are assumed to be products of the magnetization M and the complex magneto-optical coupling parameter Q. With the sample magnetization being known, the magnetic field independent Q of ferromagnetic constituents in multilayer samples can be extracted. The

*Project supported by the National Basic Research Program of China (Grant No. 2009CB929400) and the Independent Innovation Foundation of Shandong University, China (Grant No. 2012ZB040).

†Corresponding author. E-mail: opticsdu@163.com

© 2014 Chinese Physical Society and IOP Publishing Ltd

Q depends on the net spin polarization and the electronic band structure, which is very sensitive to the structural anisotropy.

By following the ideas in Ref. [6], the Jones matrix formalism is introduced in a two-dimensional coordinate system with axes parallel (index p) and perpendicular (index s) to the plane of incident. The effects of polarization and interaction of light with the magnetic material can be described by 2×2 matrices, i.e., the polarizer matrices and the reflection matrices[14]

$$\boldsymbol{R} = \begin{pmatrix} r_{\rm ss} & r_{\rm sp} \\ r_{\rm ps} & r_{\rm pp} \end{pmatrix} = r_p \cdot \tilde{\boldsymbol{R}}, \tag{2}$$

where r_{xx}, r_{xy}, r_{yx} and r_{yy} present the reflective coefficients. For longitudinal magneto-optical effects, $\tilde{\boldsymbol{R}}$, which is the reduced reflection matrix, can be written as

$$\tilde{\boldsymbol{R}} = \begin{pmatrix} \tilde{r}_{\rm s} & \tilde{\alpha} \\ -\tilde{\alpha} & 1 \end{pmatrix}, \tag{3}$$

where $\tilde{\alpha}$ is the longitudinal magnetic induced reflection coefficient and $\tilde{r}_{\rm s}$ describes the case of zero external magnetic field.

The fraction intensity change $\Delta I/I_0$ for different combinations of polarizer angles θ_1 and θ_2 for positive (+) and negative (−) directions of the external magnetic field can be written as

$$\frac{\Delta I}{I_0} = 2\frac{I_+ - I_-}{I_+ + I_-} = 4\frac{B_1 f_1 + B_2 f_2}{B_3 f_5 + 2B_4 f_4 + f_3}, \tag{4}$$

with

$$\begin{aligned} &B_1 = \Re(\tilde{\alpha}), \quad B_2 = \Re(\tilde{r}_{\rm s} \cdot \tilde{\alpha}^*), \\ &B_3 = |\tilde{r}_{\rm s}|^2, \quad B_4 = \Re(\tilde{r}_{\rm s}), \\ &f_1 = \sin^2(\theta_1)\sin(2\theta_2) - \sin^2(\theta_2)\sin(2\theta_1), \\ &f_2 = \cos^2(\theta_2)\sin(2\theta_1) - \cos^2(\theta_1)\sin(2\theta_2), \\ &f_3 = \sin^2(\theta_1)\sin^2(\theta_2), \\ &f_4 = \sin(2\theta_1)\sin(2\theta_2), \\ &f_5 = \cos^2(\theta_1)\cos^2(\theta_2), \end{aligned} \tag{5}$$

where B_i has no special meaning and is just a combination of the real or square parts of the complex parameters. The B_i can be experimentally determined by measuring $\Delta I/I_0$ for a variety of polarizer angles θ_1 and θ_2. By using the combination of B_i, the magnetically induced reflection coefficient $\tilde{\alpha}$ can be experimentally determined as

$$\tilde{\alpha} = B_1 \pm {\rm i}\frac{B_2 - B_1 B_4}{\sqrt{B_3 - B_4^2}}. \tag{7}$$

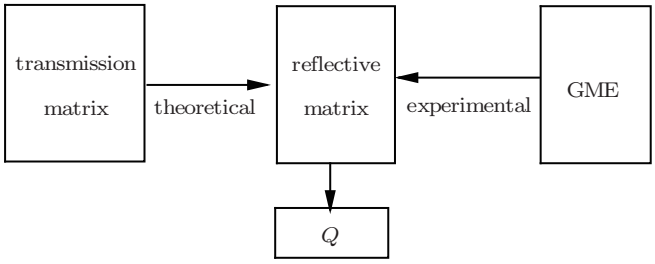


Fig. 1. Combination of GME and transmission matrix method. The reflective matrix can be obtained by experiment and theory, then the magneto-optical coupling constant Q can be found.

As shown in Fig. 1, $\tilde{\alpha}$ can be calculated in theory for ultra-thin films with different structures. In this text, the theory in Refs. [12] and [13] is introduced into the determination of the reflective matrix of the multilayer film system. The medium boundary matrices and the medium propagation matrices have been used to solve the multilayer reflection problems. Every single layer can be presented by a matrix containing its thickness and refractive index.[12] The medium boundary matrix for the i-th layer in the multilayer film system is

$$\boldsymbol{A}_i^{\rm Lon} = \begin{pmatrix} 1 & 0 & 1 & 0 \\ -\frac{1}{2}\frac{\sin\theta_i}{\cos\theta_i}(1+az_i^2)Q & \cos\theta_i & \frac{1}{2}\frac{\sin\theta_i}{\cos\theta_i}(1+az_i^2)Q & -\cos\theta_i \\ \frac{1}{2}\sin\theta_i \cdot QN_i & -N_i & \frac{1}{2}\sin\theta_i \cdot QN_i & -N_i \\ \cos\theta_i N_i & \frac{1}{2}\frac{\sin\theta_i}{\cos\theta_i}QN_i & -\cos\theta_i N_i & \frac{1}{2}\frac{\sin\theta_i}{\cos\theta_i}QN_i \end{pmatrix}, \tag{8}$$

where N_i and θ_i are the complex refractive index and the complex refractive angle of layer i, respectively. The medium propagation matrix[15] can be written as

$$\overline{\boldsymbol{D}_i} = \begin{pmatrix} u_i\cos\delta_i & u_i\sin\delta_i & 0 & 0 \\ -u_i\sin\delta_i & u_i\cos\delta_i & 0 & 0 \\ 0 & 0 & \frac{1}{u_i}\cos\delta_i & \frac{1}{u_i}\sin\delta_i \\ 0 & 0 & -\frac{1}{u_i}\sin\delta_i & \frac{1}{u_i}\cos\delta_i \end{pmatrix}, \tag{9}$$

where

$$\begin{aligned} u_i &= \exp(-{\rm i}(2\pi/\lambda)N_i\cos\theta_i d_i), \\ \delta_i &= (\pi/\lambda)N_i Q d_i \sin\theta_i/\cos\theta_i, \end{aligned} \tag{10}$$

and d_i is the film thickness. By using the medium boundary matrices and the medium propagation matrix, the single film matrix $\boldsymbol{A}_i\overline{\boldsymbol{D}}\boldsymbol{A}_i^{-1}$ for longitudinal configurations can be calculated as

$$\boldsymbol{A}_i\overline{\boldsymbol{D}}\boldsymbol{A}_i^{-1} = \begin{pmatrix} c & -\dfrac{\sin\theta_i}{2\cos\theta_i^3}Qs + \dfrac{\sigma c}{\cos\theta_i} & \mathrm{i}\dfrac{s\sigma}{N} & -\mathrm{i}\dfrac{s}{\cos\theta_i N} \\ -\dfrac{\sin\theta_i}{2\cos\theta_i}Qs - \cos\theta_i\sigma c & c & \mathrm{i}\dfrac{\cos\theta_i s}{N} & \mathrm{i}\dfrac{s\sigma}{N} \\ -\mathrm{i}sN\sigma & \mathrm{i}\dfrac{Ns}{\cos\theta_i} & c & -\dfrac{\sin\theta_i}{2\cos\theta_i^3}Qs + \dfrac{\sigma c}{\cos\theta_i} \\ -\mathrm{i}sN\cos\theta_i & -\mathrm{i}sN\sigma & -\dfrac{\sin\theta_i}{2\cos\theta_i}Qs - \cos\theta_i\sigma c & c \end{pmatrix}, \quad (11)$$

where

$$c = \cos\left(\frac{2\pi}{\lambda}Nd_i\cos\theta_i\right), \quad s = \sin\left(\frac{2\pi}{\lambda}Nd\cos\theta_i\right),$$
$$\sigma = \frac{\sin\theta_i}{\cos\theta_i}\frac{\pi}{\lambda}NQd. \quad (12)$$

For calculating the magneto-optical reflective matrix, one needs to know the $\boldsymbol{M}$ matrix. For a multilayer film, $\boldsymbol{M}$ is

$$\boldsymbol{M} = A_0^{-1}\prod_i \boldsymbol{A}_i\overline{\boldsymbol{D}_i}\boldsymbol{A}_i^{-1}\boldsymbol{A}_3 = \begin{pmatrix} \boldsymbol{G} & \boldsymbol{H} \\ \boldsymbol{I} & \boldsymbol{J} \end{pmatrix}, \quad i = 1,2, \quad (13)$$

with

$$\boldsymbol{G}^{-1} = \begin{pmatrix} t_{\mathrm{ss}} & t_{\mathrm{sp}} \\ t_{\mathrm{ps}} & t_{\mathrm{pp}} \end{pmatrix},$$
$$\boldsymbol{I}\cdot\boldsymbol{G}^{-1} = \begin{pmatrix} r_{\mathrm{ss}} & r_{\mathrm{sp}} \\ r_{\mathrm{ps}} & r_{\mathrm{pp}} \end{pmatrix}. \quad (14)$$

Then for the longitudinal magneto-optical effect, the reflective matrix of a three-layer film system (Fig. 2) can be theoretically calculated. For the ultra thin film, using Eqs. (8)–(14), we have

$$\begin{aligned} r_{\mathrm{ss}} &= [(\cos\theta_3 N_3 + \cos\theta_0)(\cos\theta_0 - N_3\cos\theta_3) \\ &\quad + 2\mathrm{i}kd_1\cos\theta_0(N_1^2\cos^2\theta_1 - N_3^2\cos^2\theta_3) \\ &\quad + 2\mathrm{i}kd_2\cos\theta_0(N_2^2\cos^2\theta_2 - N_3^2\cos^2\theta_3)] \\ &\quad \times(\cos\theta_0 + \cos\theta_3 N_3)^{-2}, \\ r_{\mathrm{sp}} &= -\frac{2k\cos\theta_0 QN_3 d_2\sin\theta_0 N_2}{(\cos\theta_3 + \cos\theta_0 N_3)(\cos\theta_0 + \cos\theta_3 N_3)}, \\ r_{\mathrm{ps}} &= -r_{\mathrm{sp}}, \\ r_{\mathrm{pp}} &= -[(\cos\theta_3 - \cos\theta_0 N_3)(\cos\theta_3 + \cos\theta_0 N_3) \\ &\quad + 2\mathrm{i}kd_1\cos\theta_0(N_1^2\cos^2\theta_3 - N_3^2\cos^2\theta_1) \\ &\quad + 2\mathrm{i}kd_2\cos\theta_0(N_2^2\cos^2\theta_3 - N_3^2\cos^2\theta_2)] \\ &\quad \times(\cos\theta_3 + \cos\theta_0 N_3)^{-2}, \\ Q &= \left(B_1 \pm \mathrm{i}\frac{B_2 - B_1B_8}{\sqrt{B_7 - B_8^2}}\right) \\ &\quad \times[(\cos\theta_0 + \cos\theta_3 N_3)((\cos\theta_3 - \cos\theta_0 N_3) \\ &\quad \times(\cos\theta_3 + \cos\theta_0 N_3) \\ &\quad + 2\mathrm{i}kd_1\cos\theta_0(N_1^2\cos^2\theta_3 - N_3^2\cos^2\theta_1) \\ &\quad + 2\mathrm{i}kd_2\cos\theta_0(N_2^2\cos^2\theta_3 - N_3^2\cos^2\theta_2))] \\ &\quad \times[2k\cos\theta_0 N_3 d_2\sin\theta_0 N_2(\cos\theta_3 + \cos\theta_0 N_3)]^{-1}. \quad (15) \end{aligned}$$

In Eq. (15), parameters B_i are obtained by the GME experiment and r_{ij} $(i,j = \mathrm{s},\mathrm{p})$ are given by reflective and transmission matrices. Through the combination of these two methods, the Q parameter formula can be obtained. The relation between Q and other parameters can be directly shown.

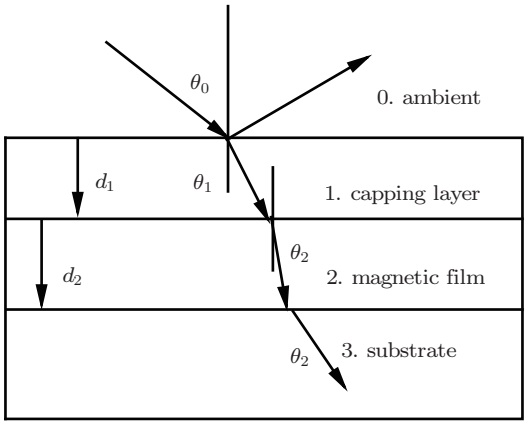


Fig. 2. Model of a three-layer system. It is composed of ambient 0, capping layer 1, magnetic film Fe and substrate GaAs. The thicknesses of the capping layer and the magnetic film are d_1 and d_2.

3. Experiment

The GME setup is modified by using a surface magneto-optical Kerr effect equipment with a laser lamp, two rotatable polarizers and a detector connected with a locked-in amplifier (Fig. 3). The un-polarized light from the laser is polarized by a polarizer P1 and then modulated by a photo chopper. After being reflected by the sample, the laser passes through analyzer P2 and is received

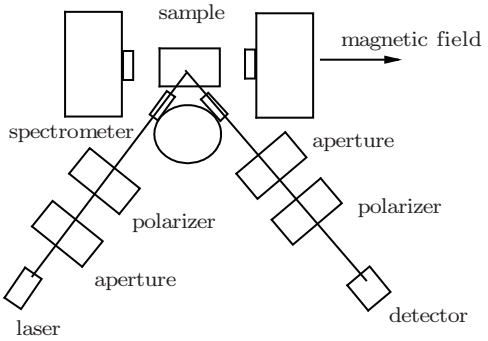


Fig. 3. Schematic diagram of GME setup. The light is polarized by a polarizer and reflected by the sample, then passes through an analyzer. The light received by the detector is processed by a locked-in amplifier to increase the SNR. After that, the signal is processed by a computer.

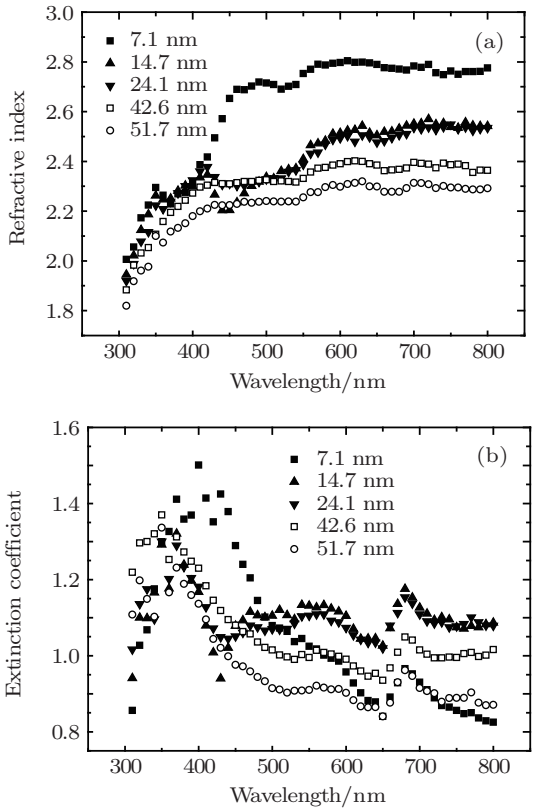


Fig. 4. Film thicknesses and optical constants ((a) refractive index and (b) extinction coefficient) of ultrathin iron films with different thicknesses.

by the detector. The signal is then processed by the locked-in amplifier. For an ultrathin film, the magnetic induced signal reflected from the sample is quite weak and the fractional intensity change is easily buried in the noise of the laser, so it is difficult to detect. So the locked-in amplifier is used here to elevate the signal to noise ratio (SNR) and extract the useful signal. The wavelength of the laser is 650 nm and the incident angle is accurately controlled at 30° by a spectrometer. The spectrometer can be used to provide an accurate incident angle in minute level after modification.[16] The external magnetic field is 250 mT, which is sufficient to produce a saturated magnetic field. The sample is placed into the center of a solenoid, which can be controlled by a programmable system. The solenoid can provide an external homogeneous saturation magnetization. The $\Delta I/I_0$ is displayed as a function of θ_2 for three different settings of θ_1.[17] The polarizer is set at 20°, 40° and 60° respectively, and the analyzer rotates from 0° to 180°. The intensity at every single analyzer angle is recorded for positive (+) and negative (−) directions of the external magnetic field.

The samples are prepared by magnetron sputtering. Surfaces of 50 mm×50 mm commercial GaAs (0 0 1) wafers are cleaned for 30 min to prepare GaAs free of any measurable contaminant. A Fe layer is then deposited at 0.7 nm/min while rotating the substrate for increased uniformity. Immediately after the Fe deposition, a Ta capping layer is deposited. Here the Ta material, which supplies the largest Kerr rotation, is the most suitable capping layer.[18] The pressure of the argon atmosphere is typically maintained at 0.9 Pa. The thicknesses of the samples are shown in Table 1.

Table 1. Thicknesses of Ta/Fe/GaAs(001) measured by spectroscopic ellipsometry.

	a	b	c	d	e
Ta/nm	10	10	10	10	10
Fe/nm	7.1	14.7	24.1	42.6	51.7

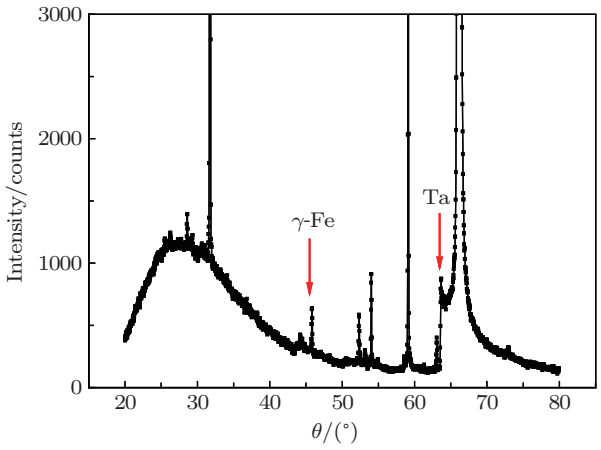


Fig. 5. (color online) XRD pattern for Ta/Fe/GaAs (sample a). The peaks of Fe and Ta are marked.

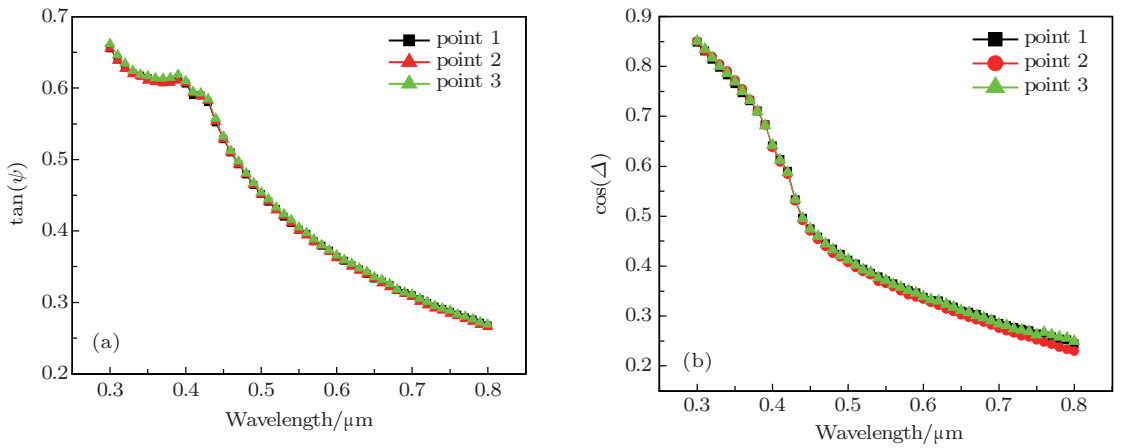


Fig. 6. (color online) The ellipsometry data ((a) $\tan(\psi)$ and (b) $\cos(\Delta)$) of sample a under wavelength 300–800 nm. These three curves represent the data of three separate points on sample a.

If the investigated multilayer sample contains thick and highly absorbing layers, the generalized ellipsometry is in general not sufficient to determine the layer thicknesses, instead other techniques would be required for such a purpose. However, the spectroscopic ellipsometry measurements and data analysis are an established method for film thickness and optical constant determination.[9] The spectroscopic ellipsometry is used to determine the optical parameter[19] (Fig. 4) and the thickness of every layer in the samples.[18] After that, the x-ray diffraction (XRD) pattern of sample a is acquired as a representation to check the quality of these samples (Fig. 5). To check the optical homogeneity, the ellipsometry data ($\tan(\psi)$ and $\cos(\Delta)$) of sample a are given by measuring three separate points of sample a (Fig. 6).

4. Results and discussion

Figure 4 shows the XRD pattern of sample a. The high peaks come from the GaAs substrate. Compared with the standard spectrum, the peaks of Ta and Fe are marked. Figure 5 displays the ellipsometry data of sample a. These three curves represent the data of three different points, which are selected randomly on sample a. From these figures, we can see that the ellipsometry data of these three different points are nearly the same, which means that the film thickness uniformity is quite good.

Figure 7 shows the fractional intensity change of the magnetic materials as a function of the analyzer angle with three curves fitted simultaneously. The R^2 shows the coefficient of determination, which describes the overall reliability of the least square fit. Table 2 lists the fitting parameters B_1–B_4 including an error estimate. It can be seen that the experiment data fit very well with the theoretical results. From this figure, we can see that the peaks increase with increasing film thickness and the $\Delta I/I_0$ under 40° is more sensitive than the other two.

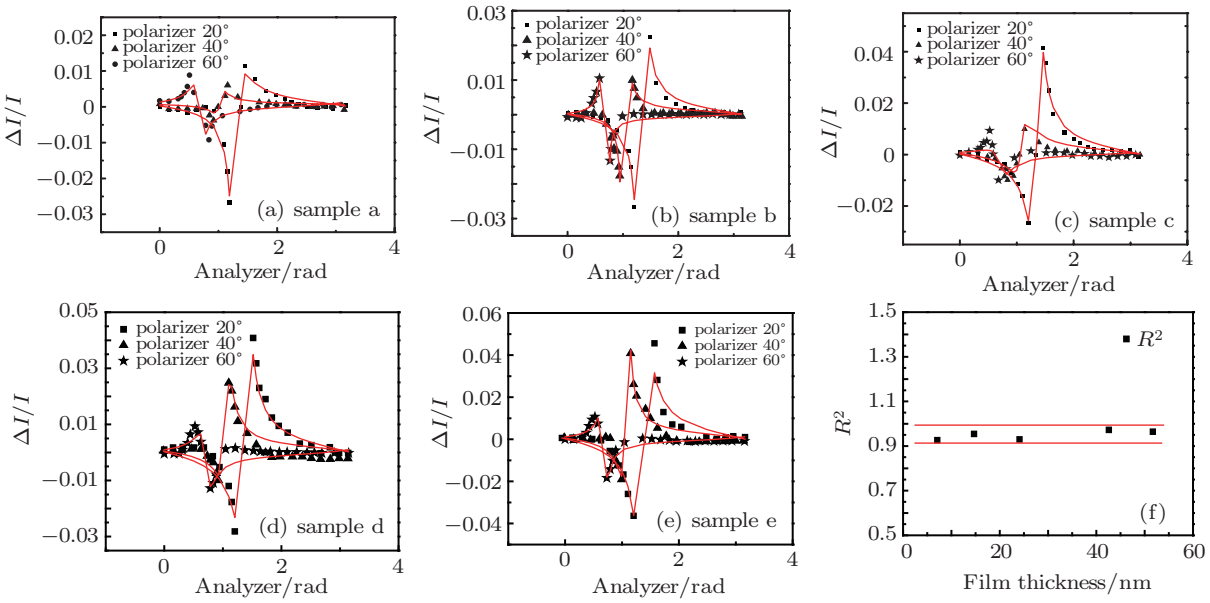


Fig. 7. (color online) Fractional intensity change of the magnetic materials ((a) sample a, (b) sample b, (c) sample c, (d) sample d, (e) sample e) as a function of the analyzer angle and (f) coefficient of determination.

Table 2. Fit parameters B_i according to the least-square fits shown in Fig. 7.

Sample		B_1	B_2	B_3	B_4
a	value	−0.00087	0.00119	1.88402	−1.3598
	error	±0.00006	±0.0001	±0.018	±0.0271
b	value	−0.00067	0.00109	2.06817	−1.44866
	error	±0.00005	±0.00007	±0.045	±0.02092
c	value	−0.00168	0.00241	2.48323	−1.51729
	error	±0.00013	±0.00013	±0.09248	±0.0348
d	value	−0.00157	0.00215	2.21486	−1.4351
	error	±0.00008	±0.00009	±0.079	±0.029
e	value	−0.00192	0.00269	2.19319	−1.47603
	error	±0.00008	±0.00012	±0.0428	±0.01437

Taking the B_i parameters into Eqs. (7)–(14), the Q parameter as a function of the Fe film thickness is given in Fig. 8. It is shown that Q as a material constant is independent of the film thickness. This conclusion is quite similar to that in Ref. [20], which uses another method named the vector-magneto-optical generalized ellipsometry. A magneto-optical Kerr rotation experiment is carried out to verify the consistence of this experiment. Figure 9 displays the experimental (symbols) and calculated (line) magneto-optical Kerr rotations and ellipticity (θ_K and ε_K) of samples a–e with different thicknesses. Using the Q value and the optical constant under 650 nm obtained from Figs. 4 and 8, the magneto-optical Kerr rotations and ellipticity are calculated. The results show that they fit well with the experiment data.

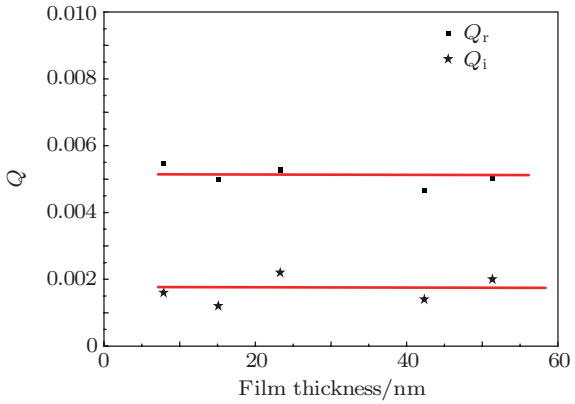


Fig. 8. (color online) Magneto-optical coupling parameters Q of samples a–f. The square and star refer to the real and imaginary parts of the magneto-optical coupling parameter.

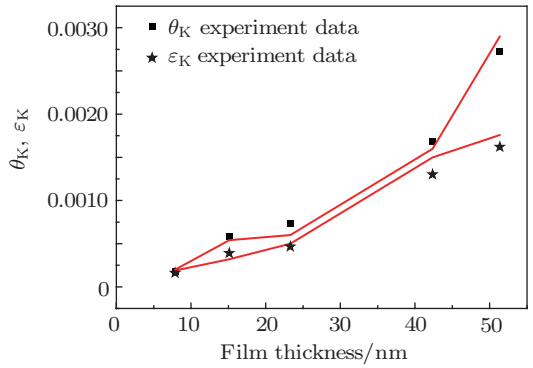


Fig. 9. (color online) Experimental (symbols) and calculated (line) magneto-optical Kerr rotations and ellipticity (θ_K and ε_K) as a function of film thickness in longitudinal configurations under 650 nm wavelength.

5. Conclusion

In this paper, the medium boundary matrices and the medium propagation matrices theories are introduced into the determination of the complex reflection matrix, then the generalized magneto-optical ellipsometry is extended to the measurement of ultrathin magnetic films. A spectroscopic ellipsometry is used to determine the optical parameters and the thicknesses of these samples. The results show that Q as a material constant is independent of the film thickness. After that, a magneto-optical Kerr rotation experiment is carried out to verify the consistence of this experiment. The theoretical curve fits very well with the experimental data.

References

[1] Bland J A C and Heinrich B 2004 *Ultrathin Magnetic Structures* (3rd edn.) (Berlin: Springer Verlag) p. 7

[2] Spoddig D, Köhler U, Haak M, Kneppe M, Schmitte T, Westphalen A, Theis-Bröhl K, Meckenstock R, You D and Pelzl J 2008 *Superlattice Microst.* **43** 180

[3] Liu L W, Dang H G, Sheng W, Wang Y, Cao J W, Bai J M and Wei F L 2013 *Chin. Phys. B* **22** 047503

[4] Yousaf M Z, Yu J, Hou Y L and Gao S 2013 *Chin. Phys. B* **22** 058702

[5] Ino Y, Shimano R, Svirko Y and Kuwata-Gonokami M 2004 *Phys. Rev. B* **70** 155101

[6] Bergera A and Pufall M R 1997 *Appl. Phys. Lett.* **71** 965

[7] Rauer R, Neuber G, Kunze J, Bäckström J and Rübhausen M 2005 *Rev. Sci. Instrum.* **76** 023910

[8] Arregi J A, Gonzalez-Diaz J B, Bergaretxe E, Idigoras O, Unsal T and Berger A 2012 *J. Appl. Phys.* **111** 103912

[9] Mok K, Du N and Schmidt H 2011 *Rev. Sci. Instrum.* **82** 033112

[10] Mok K, Kov]ács G J, McCord J, Li L, Helm M and Schmidt H 2011 *Phys. Rev. B* **84** 094413

[11] Gonzalez-Diaz J B, Arregi J A, Bergaretxe E, Fertin M J, Idigoras O and Berger A 2013 *J. Magn. Magn. Matter.* **325** 147

[12] Zak J, Moog E R, Liu C and Bader S D 1990 *J. Magn. Magn. Matter.* **89** 107

[13] Zak J, Moog E R, Liu C and Bader S D 1990 *J. Appl. Phys.* **68** 4203

[14] Metzger F, Pluvinage P and Torguet R 1965 *Ann. Phys.* **10** 5

[15] You C Y and Shina S C 1998 *J. Appl. Phys.* **84** 541

[16] Wang X, Lian J, Zhang F J, Yu X H, Li P, Gao S, Wang Y S and Sun Z Z Optik 2013 in press

[17] Azzam R M A and Bashara N M 1999 *Ellipsometry and Polarized Light* (4th edn.) (New York: Elsevier) p. 119

[18] Wang X, Lian J, Wang G T, Song P, Li P and Gao S 2011 *J. Magn. Magn. Matter.* **323** 2711

[19] Gao S, Lian J, Sun X F, Wang X, Li P and Li Q H 2013 *Chin. Phys. Lett.* **30** 027801

[20] Mok K, Scarlat C, Kovaćs G J, Li L, Zviagin V, McCord J, Helm M and Schmidt H 2011 *J. Appl. Phys.* **110** 123110